



## Formulation of multicomponent inclusion complex of cyclodextrin-amino acid with Chrysin: Physicochemical characterization, cell viability and apoptosis assessment in human primary glioblastoma cell line

Wael A. Mahdi<sup>a,\*</sup>,<sup>1</sup>, Mohammed Mufadhe Alanazi<sup>b,1</sup>, Syed Sarim Imam<sup>a,\*</sup>, Sultan Alshehri<sup>a</sup>, Afzal Hussain<sup>a</sup>, Mohammad A. Altamimi<sup>a</sup>, Sulaiman S. Alhudaithi<sup>a</sup>

<sup>a</sup> Department of Pharmaceutics, College of Pharmacy, King Saud University, Riyadh 11451, Saudi Arabia

<sup>b</sup> Department of Pharmacology and Toxicology, College of Pharmacy, King Saud University, Riyadh 11451, Saudi Arabia

### ARTICLE INFO

#### Keywords:

Chrysin  
Cyclodextrin  
L arginine  
Cell viability  
Apoptosis  
Molecular docking

### ABSTRACT

Chrysin (CR) is a water-insoluble drug reported for different therapeutic effects. The microwave irradiation method was used in this study to create a multicomponent inclusion complex (CR-MC) containing CR (drug) and carrier hydroxyl propyl beta cyclodextrin (HP  $\beta$  CD) and L-arginine (LA). The prepared inclusion complex (CR-MC) was evaluated for dissolution study and results were compared with chrysin physical mixture (CR-PM). Further, the samples were assessed for infra-red (IR), nuclear magnetic resonance (NMR), differential scanning calorimeter (DSC), scanning electron microscope (SEM) and molecular docking. Finally, the cell viability, reactive oxygen species and flow cytometer studies were also assessed to check the potential of the prepared inclusion complex on the human primary glioblastoma cell line (U87-MG cell). The phase solubility findings revealed a stability constant ( $773 \text{ mol L}^{-1}$ ) as well as a complexation efficiency of 0.027. The dissolution study displayed a significant increase in CR release from CR-MC ( $99.03 \pm 0.39\%$ ) > CR-PM ( $70.58 \pm 1.16\%$ ) > pure CR ( $35.29 \pm 1.55\%$ ). NMR and IR spectral data revealed no interaction between CR and carriers. SEM and DSC study results revealed the conversion into amorphous form. The molecular docking results illustrated a high docking score, which supports the findings of complex formation. The cell viability, reactive oxygen species, and flow cytometry studies results showed enhanced activity from CR-MC against the tested human primary glioblastoma cell line. From the results it has been observed that chrysin solubility significantly increased after complexation and there in vitro activity also enhanced against cancer cell line.

### 1. Introduction

Cyclodextrins are cyclic oligomers made from the enzymatic breakdown of starch (polysaccharide). The D-glucopyranoside units joined by glycosidic linkages make up cyclic oligosaccharides known as cyclodextrins. The multiple glucose units joined together covalently by oxygen atoms to form a hollow, truncated cone-shaped molecule. The cavity's broader rim is held together by hydrogen bonds formed between adjacent units' secondary hydroxyl groups (Brewster and Loftsson, 2007; Crini et al., 2018). Due to their hollow cone-like shapes, they can serve as hosts for lipophilic drugs, which connect to the drug molecule

through a variety of intermolecular forces (Li et al., 2011). CDs have several other benefits, like their non-toxic nature, decreased irritability, capacity to cover harsh taste and odor, and improved stability (Tiwari et al., 2010). The most extensively used naturally occurring cyclodextrin is  $\beta$ -cyclodextrin ( $\beta$  CD), which has seven glucopyranose units. The low complexation efficiency and restricted water solubility are characteristics of  $\beta$  CD (Suvarna et al., 2017). There are several chemical derivatives of natural cyclodextrins that are made by replacing some of the hydroxyl groups with other functional groups (Przybyła et al., 2020). Hydroxypropyl- $\beta$ -cyclodextrin (HP- $\beta$ -CD) is a cyclodextrin derivative that has undergone chemical modification, wherein one hydroxypropyl

*Abbreviation:* JC-1 dye, 5,5',6,6'-tetrachloro-1,1',3,3'-tetraethylbenzimidazolylcarbocyanine iodide; U87-MG cell, Human primary glioblastoma cell line; HP  $\beta$  CD, Hydroxyl propyl beta cyclodextrin; ROS, Reactive Oxygen Species; H<sub>2</sub>O<sub>2</sub>, Hydrogen peroxide..

\* Corresponding authors.

E-mail addresses: [wmahdi@ksu.edu.sa](mailto:wmahdi@ksu.edu.sa) (W.A. Mahdi), [simam@ksu.edu.sa](mailto:simam@ksu.edu.sa) (S.S. Imam).

<sup>1</sup> Wael A. Mahdi and Mohammed Mufadhe Alanazi are co-first authors and equally contributed to this work.

<https://doi.org/10.1016/j.ijpx.2023.100211>

Received 21 May 2023; Received in revised form 7 September 2023; Accepted 10 September 2023

Available online 12 September 2023

2590-1567/© 2023 The Authors. Published by Elsevier B.V. This is an open access article under the CC BY-NC-ND license (<http://creativecommons.org/licenses/by-nc-nd/4.0/>).

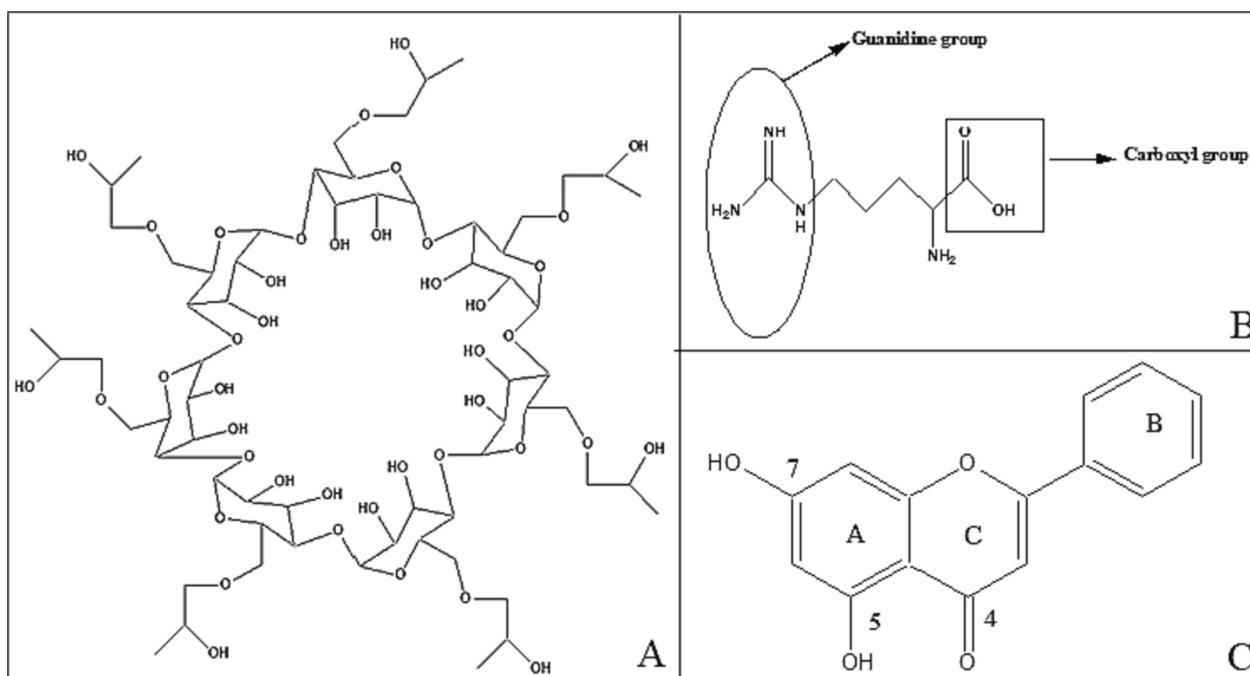


Fig. 1. Chemical structure of HP  $\beta$  cyclodextrin (A); L-arginine (B); Chrysin (C).

group replaces a hydroxyl group in each glucose unit of the host (as depicted in Fig. 1A). With a molecular weight ranging from  $\sim 1380$  to  $\sim 1460$  g/mol depending on the degree of substitution (DS), it also exhibits enhanced water solubility compared to native  $\beta$ -cyclodextrin (de Melo et al., 2016).

According to studies, auxiliary agents can assist in improving the solubility and complexation efficiency of cyclodextrin (Figueiras et al., 2010). The auxiliary agents interact with the cyclodextrin surface or the drug-cyclodextrin complex, forming aggregates or co-complexes that have higher stability constants and complexation efficiencies. The cyclodextrin content in ternary complex can be reduced by using an auxiliary substance (Suvarna et al., 2017). L-Arginine (Fig. 1B) has been used as an auxiliary component in conjugation with cyclodextrins for the improvement of poorly soluble drug solubility (Suvarna et al., 2017; Jug et al., 2014; Wang et al., 2013; Suvarna et al., 2017). The different cyclodextrin complexes using the auxiliary substance (L arginine) with the various drugs like efavirenz (Suvarna et al., 2017), nateglinide (Suvarna et al., 2017), oxapropin (Mennini et al., 2016), zaltoprofen (Sherje et al., 2018), and etodolac (Sherje et al., 2017) have been reported. They have used the different concentration of LA as auxiliary agent and reported significant effect on the enhancement in water solubility of poorly soluble drugs.

Chrysin (CR) is a water-insoluble flavonoid obtained from the Indian trumpet tree and passion flower (Fig. 1C). It is a yellow tan powder having a molecular weight of 254.24 g/mol. It is also called 5,7-dihydroxyflavone and exhibits different pharmacological activities like anti-inflammatory, antioxidant, and anticancer (Xiao et al., 2010). It has been reported to have low systemic toxicity, high nutritional value but due to low water solubility its biological activity is limited (Zhu et al., 2016; Song et al., 2020). Considering CR's safety for human use and its ability to prevent the growth of tumor cells has received the greatest interest. There is a positive correlation between consuming flavonoids and preventing cancer, as stated in the different literature (Song et al., 2020; Gonzalez and Riboli, 2010; Pan and Ho, 2008). In cell lines such as malignant gliomas (U87-MG and U-251), breast carcinoma (MDA-MB-231) and prostate cancer (PC3), it has tumor-specific effects. It showed a dose-dependent inhibition of U87-MG proliferation (Parajuli et al., 2009; Khoo et al., 2010). Considering their safety and natural

abundance, researchers are paying attention to the compounds with anti-tumor action. Furthermore, it has been shown that CR-induced cell death by induction of apoptosis level and disruption of mitochondrial membrane potential of varies cancer cells (Lim et al., 2018).

In the current study, the formation of a multicomponent inclusion complex for chrysin using HP  $\beta$  CD and LA as carrier by the microwave method. The prepared samples were evaluated for in vitro dissolution, differential scanning calorimeters, scanning electron microscope, FTIR and  $^1\text{H}$  NMR investigations. The interaction of chrysin with HP  $\beta$  CD, and LA was identified by molecular docking study. Finally, CR-MC was evaluated for cell viability, reactive oxygen species, its effects on the mitochondrial membrane potential, and apoptosis and necrosis levels using a human primary glioblastoma cell line.

## 2. Materials and methods

### 2.1. Materials

Chrysin (CR) and Hydroxypropyl  $\beta$  Cyclodextrin (HP  $\beta$  CD) were procured from Sigma Chemicals., M.O, USA. L-arginine (LA) was purchased from Loba Chemie Pvt. Ltd., Mumbai, India. Dulbecco's modified Eagle's medium (DMEM) and foetal bovine serum (FBS) were procured from Gibco, USA. All other chemicals and solvents used were of analytical grade.

### 2.2. Methodology

#### 2.2.1. Phase solubility

This study with CR, HP  $\beta$  CD, and LA was performed as per the reported method (Higuchi and Connors, 1965). This study helps to identify the effect of an auxiliary substance on the solubility and interaction of the guest (CR) with the host (HP  $\beta$  CD, and LA) (Sherje et al., 2017). This study was performed using a fixed volume of water (20 mL) and the addition of increasing concentrations of HP  $\beta$  CD (0–24 mM) with a fixed concentration of LA (0.25%). Excess CR was added gradually until a saturation stage was reached, and the flask was kept on the water bath shaker (Grant LSB18, Cambridge, UK) for 72 h at 25 °C. The samples were collected from each flask and filtered using syringe filter (0.45  $\mu\text{m}$ ).

The filtrate was measured by UV spectroscopy to estimate the CR content. Finally, the stability constant (K<sub>s</sub>) and complexation efficiency (CE) was calculated by the below formula:

$$K_c = \frac{\text{slope}}{S_0(1 - \text{slope})} \quad (1)$$

S<sub>0</sub>- Water solubility of CR without excipient.

$$CE = \frac{\text{slope}}{1 - \text{slope}} \quad (2)$$

## 2.2.2. Formulation of inclusion complex

**2.2.2.1. Physical mixture.** It was prepared by mixing weighing amount of CR-HP β CD (1:1 M) and LA (0.25% w/w). The mixture was triturated in pestle mortar for uniform mixing. The powder sample was sieved through mesh (#80), collected, and stored in tight container for further evaluation.

**2.2.2.2. Microwave irradiation method.** CR: HP β CD (1:1 M) and LA (0.25% w/w) multicomponent complex was developed by the microwave irradiation method with slight modification (Khushbu, 2022). CR was solubilized in small volume of ethanol, and separately HP β CD as well as LA were dissolved in water. Both solutions were mixed and transferred to a China dish. The sample was irradiated with microwave rays for 4 cycles (30 s/cycle) at 700 watts (Samsung MEO113M1., Malaysia). The solvent was evaporated, and the complexation was formed. Finally, the powder sample was scraped and stored for further characterization.

### 2.2.3. Dissolution study

The influence of LA in the CR-HP β CD complex was evaluated by the release study. USP Type II dissolution technique (Distek Dissolution System 2500, North Brunswick, NJ) was applied to evaluate the release behaviour. The experiment was carried out in 0.1 N HCl (900 mL) as a dissolution medium at a temperature of 37 ± 0.5 °C (Belgamwar and Kulkarni, 2017). The samples (5 mg of CR) were added to the medium with continuous stirring at 75 rpm. At a fixed time, the released samples were collected, and a fresh blank medium (5 mL) was replaced to maintain the uniform study condition. The samples were filtered and analysed for CR release at each time point using a UV spectrophotometer at 341 nm.

### 2.2.4. Infrared spectroscopy

The formation of an inclusion complex was evaluated using an IR investigation (ATR-FTIR, Bruker Alpha, Germany). The pure CR, HP β CD, LA, CR-PM, and CR-MC were examined between 4000 and 400 cm<sup>-1</sup> to check for any changes to peak position, peak shape, or peak intensity. Each sample's spectrum was compared, and the results are explained.

### 2.2.5. Nuclear magnetic resonance

It was used to assess the physical properties and structural alterations of inclusion complex and physical mixture in comparison to a pure CR. The pure CR, HP β CD, CR-PM and CR-MC were analysed at 700 MHz using an NMR instrument (Bruker NMR; software Top Spin 3.2, Switzerland). Deuterated DMSO was used as solvent for the investigation.

### 2.2.6. Differential scanning calorimetry

To assess the drug's change in nature, a differential scanning calorimetry (Mettler Toledo, Parkway Columbus, OH) study was performed on pure CR and prepared CR-MC. It gives an idea of changes in the endothermic or exothermic transformation of a pure drug after complexation. The study was performed in the temperature range of 35–400 °C, heating flow of 10 °C/min, and at a nitrogen flow rate of 20 mL/min.

### 2.2.7. Scanning electron microscope

SEM of the pure CR and CR-MC was assessed to evaluate the morphology. Gold was used to coat the prepared samples and examined under a microscope (JSM 6360A, JOEL, Tokyo Japan) to observe the changes in morphology.

### 2.2.8. Molecular docking

To confirm the formation of inclusion complex between drug and carrier, the molecular docking was performed by using the Autodock software (version 4.2) (Imam et al., 2022). The Chem3D 14.0 suite was used to draw Chrysin and L-Arginine (LA) ligand structures. The geometry optimization was performed by OPLS2005 force field. The crystal structure of β CD was extracted from PDB co-crystal of β amylase [PDB code: 1BFN, resolution 2.07 Å]. The structure of HP- β CD was manually pinched by affixing isopropyl moieties to the primary hydroxyl group (6-OH) of each glucopyranose unit of the host using the software (PyMOL-2.5.5). The software auto dock tools (ADT) version 1.5.6 ([www.autodock.scrips.edu](http://www.autodock.scrips.edu); La Jolla, CA, USA) was used to construct binary inclusion complex of Chrysin and HP- β CD cavity. Eventually, the ternary inclusion complex was stemmed by docking the binary inclusion complex with LA. The software Open Babel GUI was used to convert smiles notation into pdbqt (Protein Data Bank, Partial charge (Q) and Atom type (T) format.

### 2.2.9. Cell line study

**2.2.9.1. Cell culture.** At a concentration of 3 × 10<sup>5</sup> cells/mL, the human glioblastoma cell line (ATCC HTB-14; USA, passages 12–19) was cultured in DMEM 1; containing 10% FBS, and 1% streptomycin/penicillin (100 g/mL and 100 Unit Cells) were kept alive in a humidified incubator with flow of 5% CO<sub>2</sub> at a temperature of 37 °C. All proposed tests were done on confluent cells from passages 12 to 19. A 96-well plate was used for the experiments measuring reactive oxygen species (ROS) and the cytotoxicity assay (MTT). Complete culture medium containing FBS, streptomycin, and penicillin was used for all treatments. Every 48 h, regardless of the presence or absence of various treatments, the medium was changed.

**2.2.9.2. MTT (Cytotoxicity) assay.** Chrysin has been shown to have in vitro dose-dependent anti-malignant glioma cell action (U87-MG) (Parajuli et al., 2009). Based on mitochondrial activity, the MTT assay (Med Chem Express, USA) used to assess both cell proliferation and survival. As previously mentioned, cells were grown, collected, and trypsinized. Additionally, cells were seeded in 96-well plates with 1 × 10<sup>4</sup> cells per well (in 100 μL of media) and incubated for 24 h. Cells were tested for viability after being cultured for 24 h with pure CR, carrier (HP β CD and LA), and CR-MC. At the completion of the experiment, MTT reagent (10 μL, 5 mg/mL in PBS) was added and kept aside for 60 min. Then, DMSO (100 μL) was added, and mixture was shaken vigorously for 5 min. A microplate reader was used to detect absorbance at 570 nm.

$$\text{Cell viability (\%)} = (\text{OD of control cells} / \text{OD of treated cells}) \times 100 \quad (3)$$

**2.2.9.3. Reactive oxygen species (ROS) assay.** The study used an H2DCFDA kit (Med Chem Express, USA). Fluorogenic dye 2',7'-dichlorofluorescein diacetate is used to measure hydroxyl and ROS within the cells, also known as DCFDA or H2DCFDA. When the dye entered the cells, the cellular esterase deacetylated it into a non-fluorescent substance. The ROS then oxidized into 2',7'-dichlorofluorescein (DCF- a highly fluorescent chemical (excitation 485 nm and emission 535 nm). The cells were cultured (3 × 10<sup>5</sup> cells/mL) in 96-well plates for 24 h. The middle range effective concentration for this experiment was used to incubate cells with various concentrations of pure CR, CR-MC, and H<sub>2</sub>O<sub>2</sub> (positive control) for 4 h.

**2.2.9.4. Mitochondrial membrane potential measurement.** The effects of

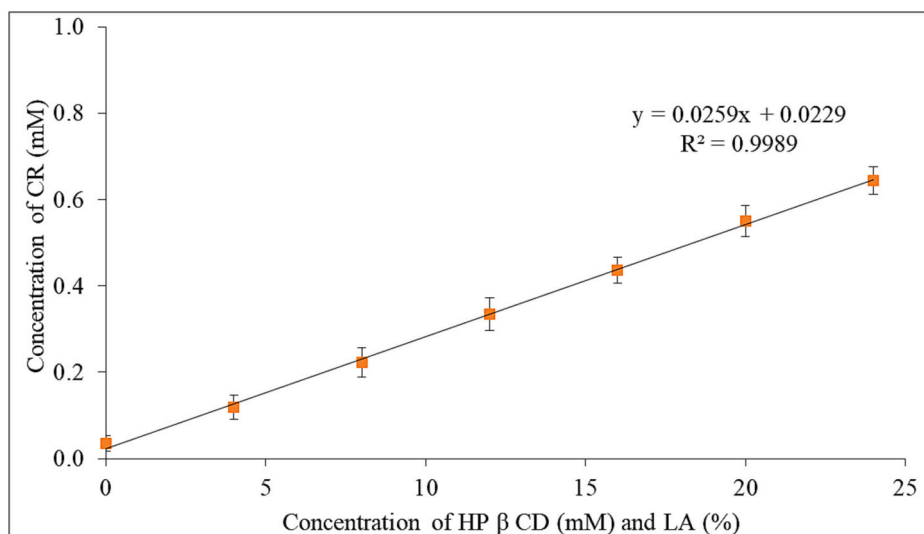


Fig. 2. Phase solubility study result of Chrysin – HP  $\beta$  cyclodextrin with L Arginine. Experiments were performed in triplicate ( $n = 3$ ).

pure CR, carrier, and CR-MC on mitochondrial function were conducted utilizing JC-1 dye. JC-1 dye is used as an indicator of mitochondrial membrane potential; JC-1 dye exists as a monomer that accumulates in mitochondria. In non-apoptotic cells, JC-1 accumulates as aggregates resulting in red fluorescence. JC-1 exists in the green, fluorescent monomeric form in apoptotic cells with diminished mitochondrial membrane potential. The cells were cultured ( $3 \times 10^5$  cells/mL) in 96-well plates for 24 h. After this stabilization period, cells were incubated with different concentrations of pure CR, CR-MC (1, 5, 10  $\mu$ M), and  $H_2O_2$  (positive control) for 24 h. Subsequently, we followed the manufacturer's instruction to evaluate the effects of pure CR, carrier, and CR-MC on mitochondrial membrane potential.

**2.2.9.5. Flow cytometry.** Viability of U87-MG cell lines were tested by flow cytometry analysis after treatment with different concentrations of pure CR, carrier, and CR-MC. Cells were culture in 6-well culture plates until 80% confluence is reached, and then treated with pure CR, carrier, and CR-MC at 10  $\mu$ M concentration, respectively. After the incubation periods, cells were trypsinized and washed with PBS, using a Beckman

refrigerated centrifuge at 1000 rpm. The pellets were incubated in ice (1 h), then centrifuged and re-suspended in Annexin-V/7-PI binding buffer (400  $\mu$ L). The cells (100  $\mu$ L,  $1 \times 10^5$ ) were re-suspended and transferred to FACS tubes and added with PE Annexin V and PI (5  $\mu$ L). The samples were vortexed and incubated at room temperature for 15 min. Finally,  $1 \times$  binding buffer were added and analysed by flow cytometer within 1 h of preparation using flow cytometer (BD C6 Accuri, BD Biosciences).

#### 2.2.10. Statistical analysis

Results are presented as mean  $\pm$  SEM. All statistical analyses were performed using One-way Anova followed by Tukey post hoc test with the level of significance set at  $P < 0.05$ . Statistical analysis was achieved using GraphPad Prism v. 8 (CA, USA) (Fatani et al., 2023).

### 3. Results and discussion

#### 3.1. Phase solubility

To know the mechanisms of drug solubility in water, a phase-

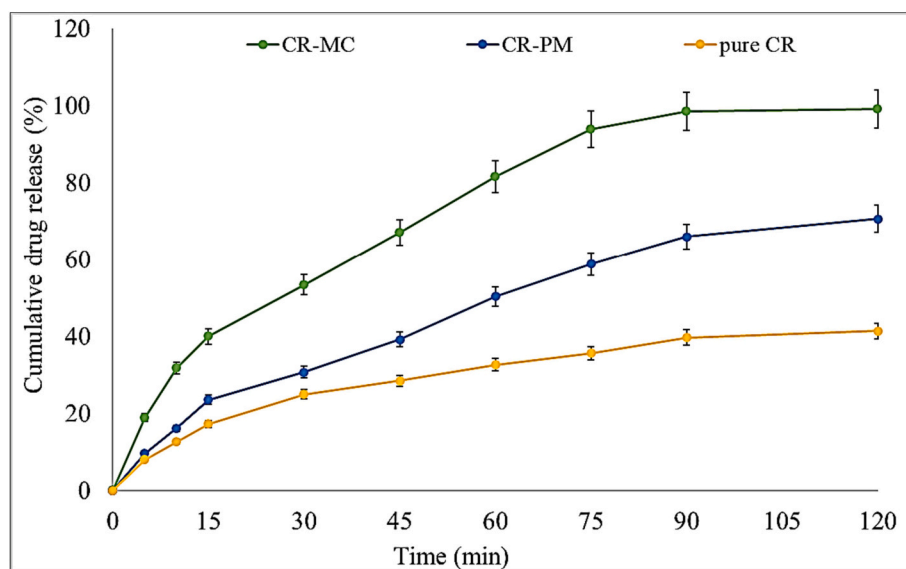


Fig. 3. In vitro dissolution study of pure chrysin (CR), chrysin physical mixture (CR-PM) and chrysin inclusion complex (CR-MC). Study performed in triplicate ( $n = 3$ ) and data depicted as mean  $\pm$  SD.

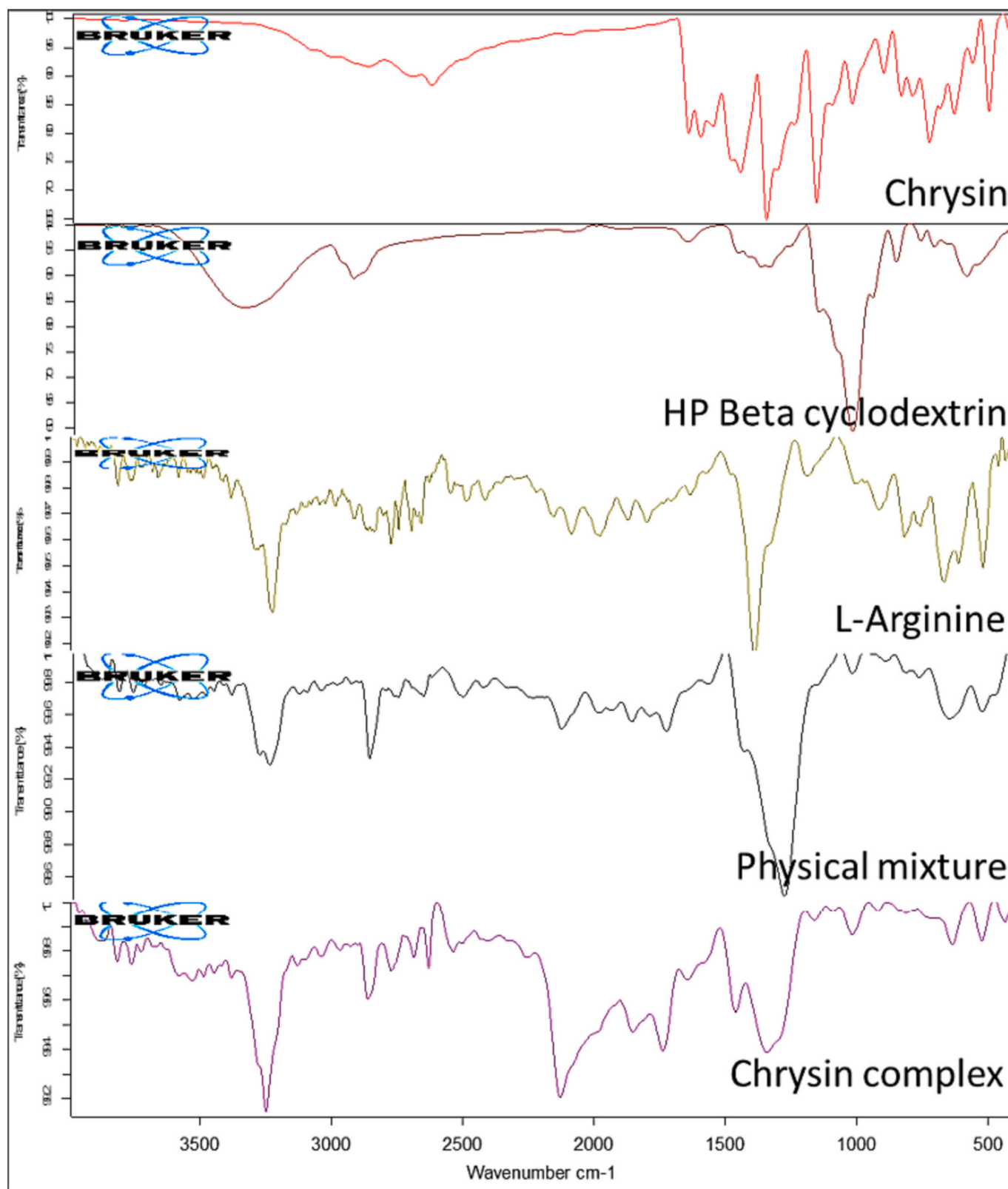


Fig. 4. IR spectra of pure chrysin (pure CR), HP  $\beta$ CD, L arginine, chrysin physical mixture (CR-PM) and chrysin multicomponent complex (CR-MC).

solubility experiment of CR in HP  $\beta$  CD and LA was conducted. The findings of this assessment demonstrated the role of LA in the solubility of CR in the presence of HP  $\beta$  CD (Fig. 2). The addition of an auxiliary substance interacts with the CD outer surface as well as with drug-CD complexes to form co-complexes that display higher stability constant

( $773 \text{ mol L}^{-1}$ ) and complexation efficiency of 0.027 than binary system (Imam et al., 2022). In our previous research we have evaluated the binary (chrysin-HP  $\beta$ CD) and ternary inclusion complex (chrysin-HP  $\beta$ CD-poloxamer). The different research also reported the stability constant value of CR with different CDs in the range of  $275$  to  $1200 \text{ M}^{-1}$ .

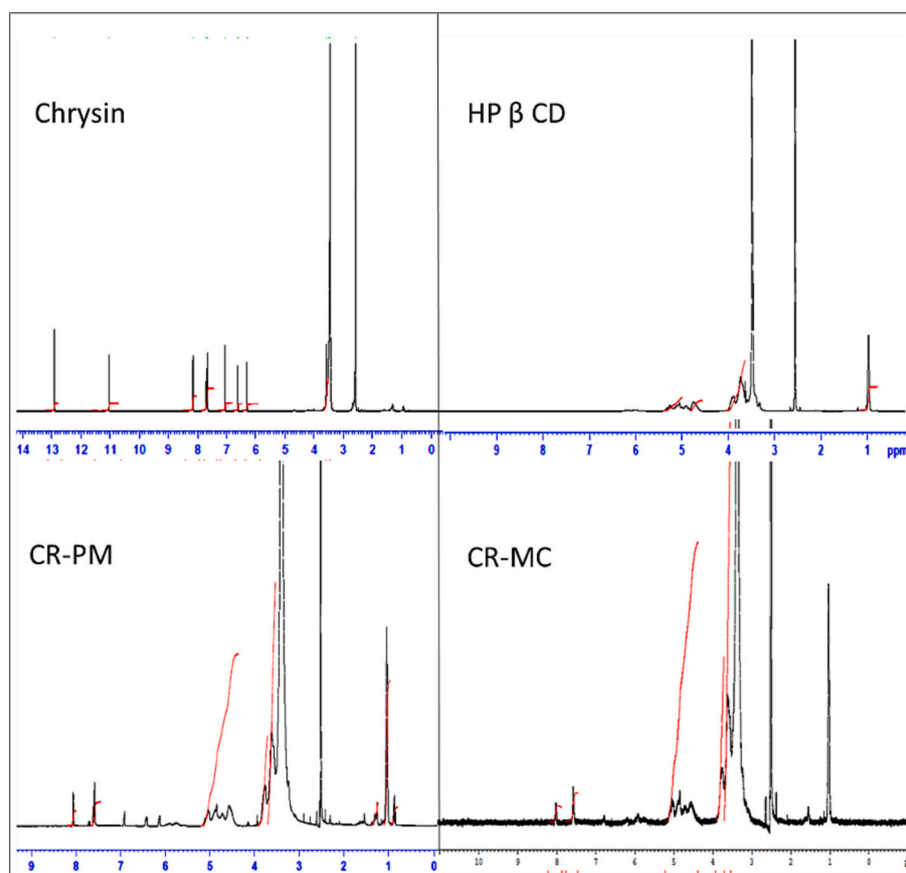


Fig. 5. NMR spectra of pure chrysin (pure CR), HP  $\beta$  CD, chrysin physical mixture (CR-PM) and chrysin multicomponent complex (CR-MC).

Our study finding was found to be within reported range (Lavania and Garg, 2023; Fenyvesi et al., 2020). It helps to enhance the CE and allow the use of low quantity of CD. The stability constant value between 100 and 1000 mol L<sup>-1</sup> found to be stable. The value >100 mol L<sup>-1</sup> indicates a highly unstable complex, whereas the value <1000 mol L<sup>-1</sup> may impair drug absorption (Suvarna et al., 2017; De Miranda et al., 2011). The phase solubility graph found to be of A<sub>L</sub> type, a linear rise in solubility with increase in HP  $\beta$  CD concentration. The electrostatic interaction of LA with the drug and HP  $\beta$  CD may be responsible for the considerable improvement in the stability constant of CR. LA interacts simultaneously with drugs via salt formation and electrostatic interaction and with cyclodextrin via hydrogen bonding (Mura et al., 2005). According to phase solubility experiments, LA has increased the rate of complex formation in addition to improving the efficiency with which HP  $\beta$  CD complexes with CR.

### 3.2. Dissolution study

The pure CR, CR-PM, and CR-MC were studied to determine the change in release behaviour of CR after complexation. Fig. 3 shows the release profile as follows: pure CR (35.29  $\pm$  1.55) > CR-PM (70.58  $\pm$  1.16) > CR-MC (99.03  $\pm$  0.39). The poor release of CR was found to be due to its poor water solubility. The physical mixture demonstrated significantly ( $p < 0.05$ ) improved drug release because of partial inclusion into the HP  $\beta$  CD, as well as the presence of LA, which also aids in solubilization. The chrysin multicomponent complex (CR-MC) showed significantly enhanced CR release from the initial time point. At 10 min interval, it showed the CR release of 31.73  $\pm$  2.71%. The maximum CR release of 98.48  $\pm$  0.39% was achieved at 90 min. A non-significant change in the release was found at 120 min (99.03  $\pm$  0.39%). In the case of a pure drug, it showed only 12.58  $\pm$  0.39% in 10 min, and the

maximum release of 35.29  $\pm$  0.71% was found after 120 min of study. The physical mixture (15.32  $\pm$  2.71%) released about 3% more CR in the initial 10-min study, but a significant ( $p < 0.05$ ) increase in release (about 35%) was achieved after 120 min of study (70.58  $\pm$  1.16%) compared to pure CR. A significant increase in drug release was found due to the inclusion of CR in HP  $\beta$  CD in presence of LA. When the CR and LA interact, the CR serves as a counter-ion and could even create an amphiphilic structure. It consists of a polar head that has hydrophilic portion and the hydrophilic portion LA attach to the drug and CD. It acts as a surfactant and lowers the aqueous surface tension and enhancing its wettability, solubility, and dissolution (Suvarna et al., 2018; Sherje et al., 2017; Mura et al., 2005). Due to the possibility for the basic amino acid to simultaneously interact with the drug and CD through electrostatic interactions and salt production (Barillaro et al., 2004), it increases the HP  $\beta$  CD solubilizing potency towards CR. It has a variety of hydrophilic moieties and can interact with the hydroxyl groups on the outside of CD by creating hydrogen bonds with them. It also acts as a cross-linker between the guest and CD, enhancing complex stability (Redenti et al., 2001).

### 3.3. Infra-red spectroscopy

Fig. 4 shows the assigned frequency for the pure CR, LA, HP  $\beta$  CD, CR-PM and CR-MC. The hydroxyl stretching vibration of CR, also known as 5,7-dihydroxyflavone, is clearly visible at 2867.74 cm<sup>-1</sup>, and the aromatic C=C bending peak is at 1646.94 cm<sup>-1</sup>. The stretching vibrations for the carbonyl (C=O) group also were visible in the spectra, peaking at 1601.79 cm<sup>-1</sup> and 1449.69 cm<sup>-1</sup>, respectively. The stretching vibrations of the O-H and C-O-C moiety are represented by the carrier HP  $\beta$  CD at 3341.09 and 1016.32 cm<sup>-1</sup>. LA showed characteristic peaks at 3428.14 cm<sup>-1</sup> (1<sup>o</sup> amine stretching), 3231.61 cm<sup>-1</sup> (2<sup>o</sup> amine stretching), and

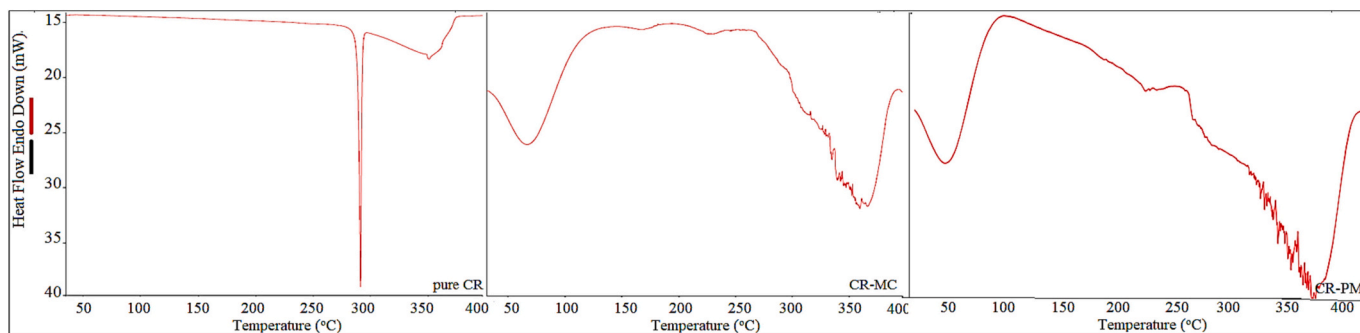


Fig. 6. DSC thermogram of pure chrysin (pure CR) and chrysin multicomponent component (CR-MC) and chrysin physical mixture (CR-PM).

2903.14  $\text{cm}^{-1}$  for -COOH stretching. Conversely, the CR-PM, exhibited slight change in peaks at 1650.42  $\text{cm}^{-1}$  for C=C aromatic bending. It was observed that there was no carbonyl (C=O) stretching vibration peak for pure CR. This observation was also in compliance with  $^1\text{H}$ NMR spectral findings. Pyran ring exhibited slight change in its vibrational peak at 1457.56  $\text{cm}^{-1}$  as compared to the pure CR. The slight change in the characteristic peaks for 1° and 2° amine of the carrier LA was also observed at 3405.17 & 3216.61  $\text{cm}^{-1}$ . The carboxylic peak of the LA was observed at 2909.52  $\text{cm}^{-1}$ . The slight change in -OH group peak for HP  $\beta$  CD was observed at 3330.46  $\text{cm}^{-1}$ . A slight change in the peak for C-O-C

stretching vibration of HP  $\beta$  CD exhibited at 1037.28  $\text{cm}^{-1}$ . In case of CR-MC, the broad -OH peaks and carbonyl group peaks of pure CR were absent, which was also in agreement with  $^1\text{H}$  NMR spectra. The Pyran ring peak of the pure CR were observed with slight change in the value at 1448.62  $\text{cm}^{-1}$ . The change in the peaks values of the carriers were also observed. LA peaks for 1°, 2° and carboxylic acid were observed at 3519.85, 3260.86 and 2916.78  $\text{cm}^{-1}$ , respectively. The carrier peaks of HP  $\beta$  CD were also observed with a significant change in their peak's values at 3392.38 and 1080.27  $\text{cm}^{-1}$  for hydroxyl and -C-O-C functional group. The change in the spectral peaks, seems to confirm that there is a

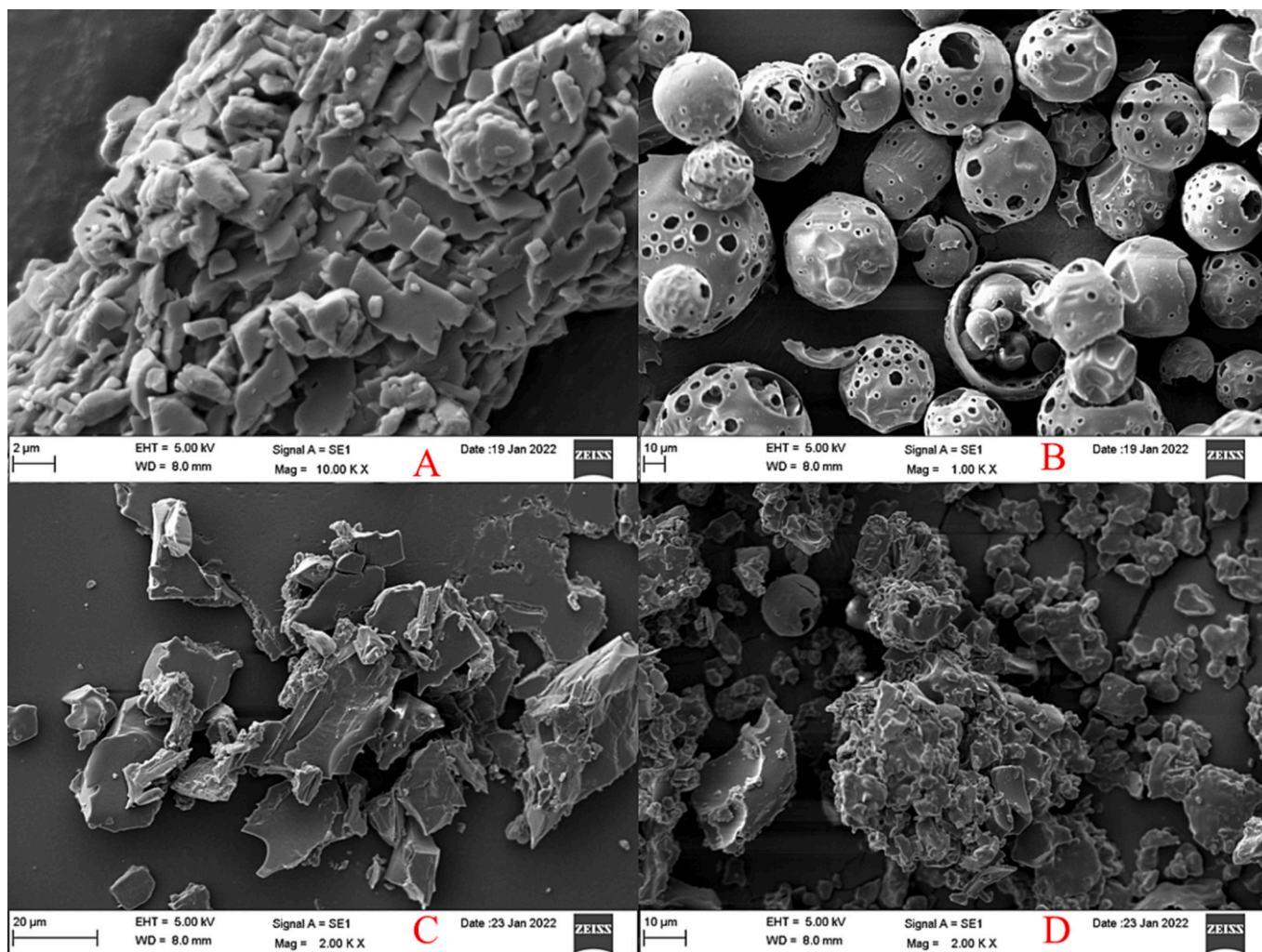
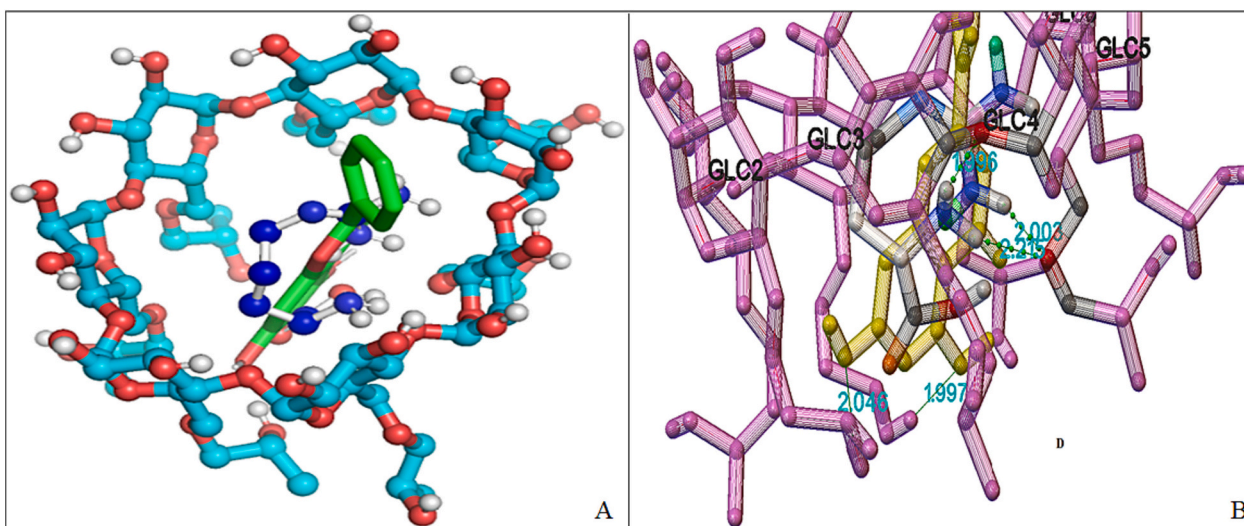


Fig. 7. Scanning electron microscope image of (A). pure chrysin; (B). HP  $\beta$  CD; (C). chrysin physical mixture (CR-PM); (D). chrysin multicomponent complex (CR-MC).



**Fig. 8.** (A). Molecular docking image (ball and stick model) of chrysin (Green) and L arginine (blue) with HP  $\beta$  cyclodextrin (cyan), (B). Chrysin formed two H-bond at GLC 1 (2.046 Å) and GLC 3 (1.997 Å) of HP  $\beta$ CD. L Arginine formed 3H bonds at GLC 4 (1.996 Å) and GLC 5 (2.215 Å and 2.003 Å).

formation of CR-MC. The above findings were also confirmed by  $^1\text{H}$ NMR spectral values and molecular docking evaluation.

### 3.4. Nuclear magnetic resonance

To determine the complex formation,  $^1\text{H}$  NMR of pure CR, carriers (LA and HP  $\beta$  CD), and developed samples (CR-PM & CR-MC) were also studied (Fig. 5). The deshielded singlet peak at 12.83 and 10.96 ppm can be attributed to the OH proton of flavonoids at C-5 and C-7. At about 8.09 ppm, the pyran ring showed a singlet peak. In the carrier LA, discrete deshielded guanidine peaks were observed between 3.38 and 3.52 ppm. At position 1 of the glucose moiety, the singlet peak for the HP  $\beta$  CD was detected at a concentration of 5.04 ppm. It was also possible to see the other peaks of the glucose moiety. The hydroxyl moiety of HP  $\beta$  CD has a singlet peak that may be seen at 3.78 ppm. The C-5 and C-7 hydroxyl of the flavonoid aromatic ring are not clearly visible in the CR-PM as a deshielded singlet. Additionally, it showed an 8.06 ppm pyran ring singlet peak. When compared to the pure CR peaks, the above alterations to the proton NMR peaks are negligible. The carrier's deshielded peak was clearly visible, and a notable change at 3.38–3.62 ppm showed the carrier's guanidine peak. The glucose moiety at position 1 in the CR-PM contained the singlet peak for the HP  $\beta$  CD carrier at a concentration of 5.04 ppm. The developed CR-MC also showed that C-5 and C-7 OH proton of the pure CR was not present. At 8.02 ppm, the chemical shift of the pyran ring underwent a small alteration. CR-MC displayed the deshielded LA peaks at 3.36–3.62 ppm, which are attributed to the carrier's guanidine proton. At position 1 of the glucose moiety, the singlet peak for the HP  $\beta$  CD carrier was investigated at a concentration of 5.04 ppm. The spectrum values coincided with IR spectral values, demonstrating that the drug and carriers form a multicomponent complex.

### 3.5. Differential scanning calorimeter

DSC was performed to characterize and confirm the complex formation of pure CR with HP  $\beta$  CD, and LA (Fig. 6). The pure CR revealed a pronounced endothermic peak at 291.2 °C, which is comparable to the drug melting point (Song et al., 2020). In case of CR-MC, the endothermic peak disappeared from the DSC profile, which may be due to the enhanced interaction/solubilization with HP  $\beta$  CD and LA. The fact that only the endothermic effects of dehydration at 69.2 °C and decomposition after 300 °C were noticed suggests that all the components interacted completely. A strong indication of the formation of a more

amorphous entity in the multicomponent complex is due to the loss of the pure CR endotherm peak.

### 3.6. Scanning electron microscope

The findings of the investigation using scanning electron microscopy showed the shape of pure CR changed after formation of inclusion complex (Fig. 7). The images were captured for pure CR, HP  $\beta$  CD, CR-PM, and CR-MC. The pure CR appeared as thin, elongated crystal aggregates in Fig. 7A, whereas HP  $\beta$  CD appeared as 3D globular-shaped particles (Fig. 7B) (Ribeiro et al., 2003). Due to the partial inclusion of CR in the HP  $\beta$  CD, and LA, the physical mixture structure has changed. In the micrographs, a few recognisable elements may be seen (Fig. 7C). The multicomponent inclusion complex only exhibits one component (Fig. 7D) (da Silva Mourao et al., 2016). The morphology differed significantly from the physical mixture. The distinctive amorphous structure of smaller dimensions than those found in the pure drug has replaced the patterns of CR crystals and HP  $\beta$  CD. These morphological and crystallographic alterations offer compelling proof that inclusion complexes have formed. The surfaces were irregular, porous and were composed of homogeneous, amorphous agglomerates. It is interesting that the amorphous material would dissolve more quickly than the crystalline counterpart due to its higher internal energy and molecular mobility (Bera et al., 2016). As a result of a change in crystalline habitus in the multicomponent systems upon complexation, the change in particle shape indicates the development of a new solid phase (Sami et al., 2010).

### 3.7. Molecular docking

The molecular docking research provided additional insight into the stability of the inclusion complex formation as shown in Fig. 8. It is utilized to interpret the molecular configuration of pure CR, HP  $\beta$  CD and LA. AutoDock 4.2 with Lamarckian genetic algorithm determined the proper binding modes and confirmed the ligand. Fig. 8A depicts the docking of the pure ligands CR and LA with the HP  $\beta$  CD. The pure CR and HP  $\beta$  CD were found to have a binding affinity score of -6.51 kcal/mol. The binding interaction was depicted by forming two hydrogen bonds at C-5 & C-7 hydroxyl moiety of the flavonoid with GLC 3 and GLC 1 of HP  $\beta$  CD with the bond length of 1.997 Å and 2.046 Å, respectively (Fig. 8B). This elucidates the host-guest (ligand) interaction forming the binary complex. The ternary inclusion complex was also executed with the software by docking LA (auxiliary agent) with the pure CR- HP  $\beta$  CD

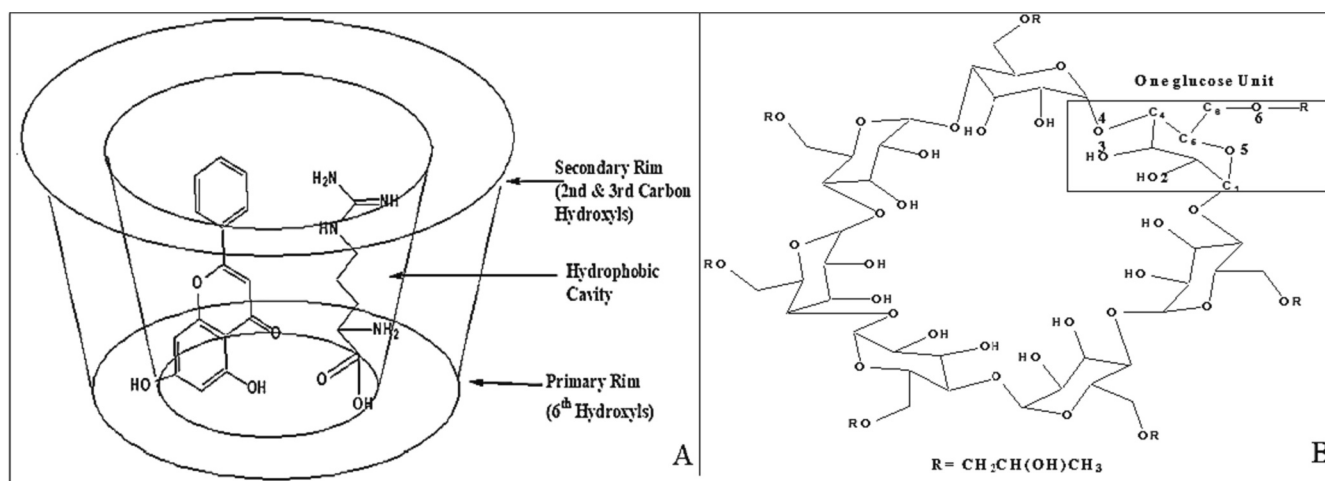


Fig. 9. (A). Position of chrysin (guest) and L-arginine (auxilliary agent) with respect to cyclodextrin (host); (B). Labelling of 1 glucose unit of HP  $\beta$  cyclodextrin.

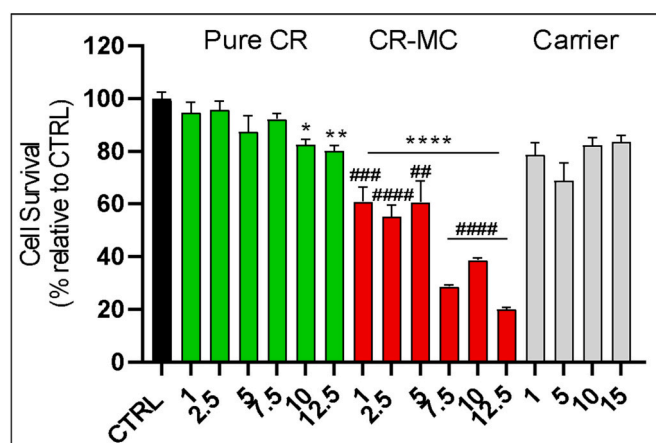


Fig. 10. Evaluation the effects of pure chrysin (CR in  $\mu\text{M}$ ), chrysin multicomponent complex (CR-MC in  $\mu\text{M}$ ) and carrier (HP  $\beta$  CD + LA in  $\mu\text{M}$ ) on U87-MG cells viability after 24 h treatment. Study performed in quadruplet and data shown as mean  $\pm$  SEM. \* Comparison with control; # Comparison with pure chrysin at same dose.

binary complex. The binding affinity score of LA with respect to CR-HP  $\beta$  CD was found to be  $-3.78$  kcal/mol (Fig. 8A). The aliphatic guanidine side chain was found to be present towards secondary rim of HP  $\beta$  CD. According to the molecular interaction studies of LA, the carboxyl moiety was found to be present at GLC 4 of the HP  $\beta$  CD. The auxiliary agent (LA) formed three hydrogen bonds at GLC 4 and GLC 5 of HP  $\beta$  CD with the bond length of 1.996, 2.215 & 2.003 Å, respectively (Fig. 8B). No steric hindrance was observed between pure CR (guest) and LA (auxiliary agent) while forming the binary and ternary inclusion complex when arranged at CD's hollow cavity. It demonstrates that the pure CR and LA were aligned in the CD's hollow center towards the primary rim of CD's truncated cone (Fig. 9A-B). The primary rim of HP  $\beta$  CD was occupied by the flavonoid ring of CR. The aromatic ring of the pure drug occupies hollow CD towards the secondary rim. The produced multicomponent inclusion complex may be regarded as thermodynamically stable, according to the above observations.

No steric hindrance was observed between pure CR (guest) and LA (auxiliary agent) while forming the binary and ternary inclusion complex when arranged at CD's hollow cavity. It demonstrates that the pure CR and LA were aligned in the CD's hollow center towards the secondary rim of CD's truncated cone (Fig. 9A-B). The Pyran ring of the pure drug occupies hollow CD towards the secondary rim. The Primary rim of HP  $\beta$

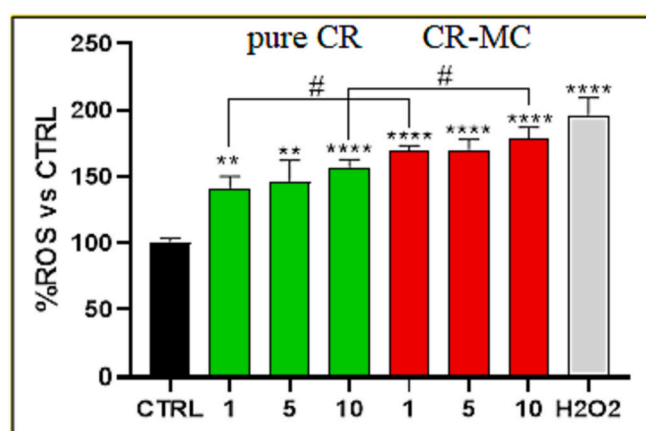


Fig. 11. Evaluation the effects of pure chrysin (CR in  $\mu\text{M}$ ), chrysin multicomponent complex (CR-MC in  $\mu\text{M}$ ) and standard ( $\text{H}_2\text{O}_2$  in  $\mu\text{M}$ ) on reactive oxygen species (ROS) generation after 4 h treatment. Study performed in quadruplet and data shown as mean  $\pm$  SEM.

CD was occupied by the aromatic flavonoid ring of CR. The produced multicomponent inclusion complex may be regarded as thermodynamically stable, according to the above observations.

### 3.8. Cell viability

The study of pure CR, carrier, and CR-MC was evaluated against a human primary glioblastoma cell line. The comparative data is shown in Fig. 10. The study was performed in the concentration range of 1–12.5  $\mu\text{M}$ . The results showed concentration-dependent activity against the cell line. As the concentration of CR increases, the cells viability decreases. The carrier showed slight effect on the tested cell line. Its effect was not found to be significant. HP  $\beta$  CD has been reported for its anticancer activity against different cancer cell lines (Yokoo et al., 2015). The pure CR displayed less activity than the CR-MC. At an initial 1  $\mu\text{M}$  concentration, the pure CR showed 94.6% cell viability, whereas the CR-MC depicted highly significant ( $p < 0.001$ ) cell viability (60.86%). At the tested concentrations, there was a difference in activity of 2.5 M (95.7%, ns), 5 M (87.4%, ns), 10 M (82.6%,  $p < 0.05$ ), and 12.5 M (80.5%,  $p < 0.01$ ). But in the case of the prepared formulation CR-MC, at concentrations of 2.5  $\mu\text{M}$  (55.1%,  $p < 0.001$ ), 5  $\mu\text{M}$  (60.3%,  $p < 0.001$ ), 7.5  $\mu\text{M}$  (28.5%,  $p < 0.0001$ ), 10  $\mu\text{M}$  (38.3%,  $p < 0.0001$ ) and 12.5  $\mu\text{M}$  (20.1%,  $p < 0.001$ ) in comparison to the control. A significant change in activity was observed at all concentrations. It works as an

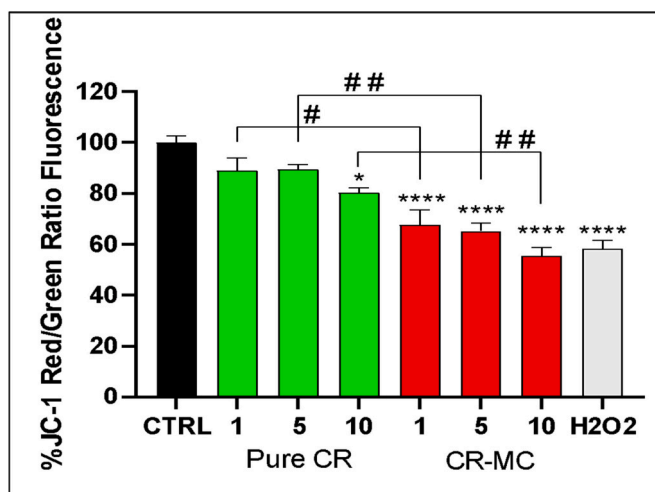


Fig. 12. Evaluation the effects of pure chrysin (CR in  $\mu\text{M}$ ), chrysin multicomponent complex (CR-MC  $\mu\text{M}$ ) and standard ( $\text{H}_2\text{O}_2$  in  $\mu\text{M}$ ) on mitochondrial membrane potential after 24 h treatment. Study performed in quadruplet and data shown as mean  $\pm$  SEM. \* Comparison with control; # Comparison with pure chrysin at same dose.

anticancer agent by activating caspases and inhibiting Akt signalling. It also inhibits cancer cell proliferation and induces apoptosis. It is more active than other flavonoids in cancer cells (Khoo et al., 2010). Our results indicated that, both pure CR and CR-MC have decreased U87-MG cells viability significantly in a dose-dependent manner compared to the control groups. Interestingly, with all doses, the prepared CR-MC reduced the U87-MG cells viability significantly in comparison to the

matched doses in the pure chrysin groups. Furthermore, our results also showed that the carrier that has been used for the preparation of the inclusion complex has almost no effect on the U87-MG cell viability.

### 3.9. Reactive oxygen species (ROS) assay

The study results described that both pure CR and CR-MC have significantly increased ROS generation in U87-MG cells compared to the control group (Fig. 11). Interestingly, concentrations of 1 and 5  $\mu\text{M}$  (CR-MC) significantly increased ROS generation in U87-MG cells when compared to matched concentrations of pure CR groups.  $\text{H}_2\text{O}_2$  was used as a positive control to induce ROS generation.

### 3.10. Mitochondrial membrane potential measurement

Our study has demonstrated that all the used concentrations of CR-MC have induced mitochondrial dysfunction significantly compared to non-treated cells ( $P < 0.0001$ ). On the other hand, only the concentration 10  $\mu\text{M}$  of pure CR has induced mitochondrial dysfunction significantly compared to non-treated cells ( $P < 0.05$ ). Interestingly, the concentrations of 1, 5, and 10  $\mu\text{M}$  (CR-MC) significantly decreased the mitochondrial membrane potential in U87-MG cells when compared to the matched concentrations of pure CR groups ( $P < 0.01$ ,  $P < 0.001$ , and  $P < 0.001$ , respectively).  $\text{H}_2\text{O}_2$  was used as a positive control to induce the mitochondrial dysfunction (Fig. 12).

### 3.11. Flow cytometry

Our study has shown that 10  $\mu\text{M}$  of either pure CR and CR-MC has increased apoptosis levels significantly compared to the control group ( $P < 0.01$  and  $P < 0.0001$ , respectively). Interestingly, incubation of

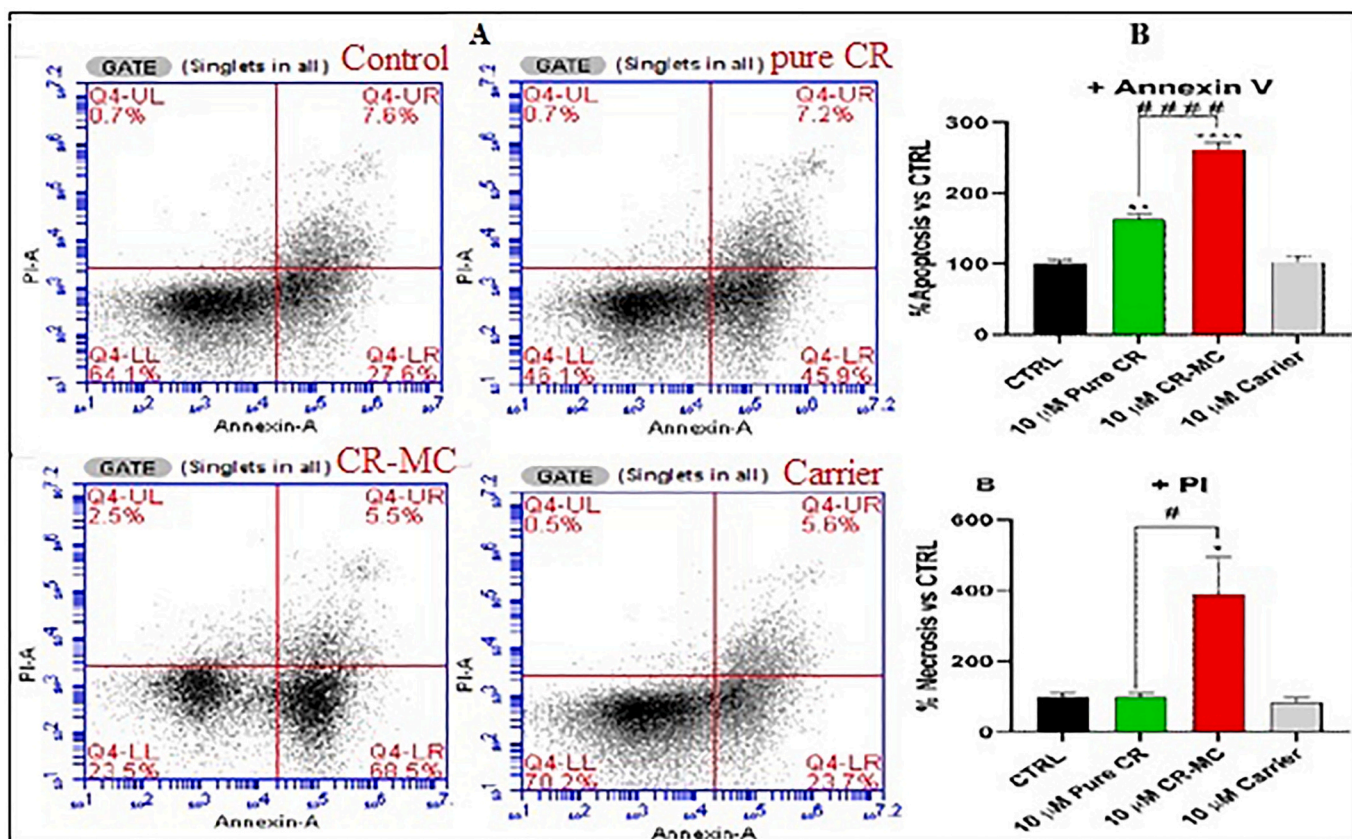


Fig. 13. Evaluation the effects of Control, pure chrysin (CR), chrysin multicomponent complex (CR-MC) and carrier on apoptosis (A) and necrosis (B) levels after 24 h treatment. Study performed in Triplicate and data shown as mean  $\pm$  SEM. \* Comparison with control; # Comparison with pure chrysin at same dose.

cells with 10  $\mu\text{M}$  CR-MC has increased the apoptosis levels significantly compared to the matched concentration of pure CR ( $P < 0.0001$ ) (Fig. 13A). Levels of necrosis have been increased significantly only in cells treated with CR-MC (10  $\mu\text{M}$ ), but not with pure CR, compared to the control groups ( $P < 0.05$ ). Carrier has demonstrated comparable effects on apoptosis and necrosis levels in compared to the control group. Interestingly, 10  $\mu\text{M}$  (CR-MC) significantly increased the necrosis level in U87-MG cells when compared to the matched concentration of pure CR groups ( $P < 0.05$ ) (Fig. 13B).

#### 4. Conclusion

The multicomponent complex of CR with HP  $\beta$  CD and LA was performed by using microwave irradiation method. The prepared complex was characterized for different parameters and cell viability study. It showed higher stability constant value which confirms the formation of stable complex at the used ratio. A significant increase in the drug release was achieved from CR-MC. The solid state and liquid state characterization results depicted formation of complex due to the change in the characteristics of pure CR after complexation. The cell line study results revealed the chrysin inclusion complex has the significantly better in vitro activity against glioblastoma cell line. Our study has shown CR-MC decreased U87-MG cell viability, increased ROS generation, decreased mitochondrial membrane potential, and increased apoptosis and necrosis levels significantly compared to the matched doses of pure CR. From the study, it has been concluded that the enhancement of solubility of poor soluble chrysin achieved after formation of inclusion complex using HP  $\beta$ CD and LA. It leads to get better activity than pure drug.

#### CRedit authorship contribution statement

**Wael A. Mahdi:** Supervision, Visualization. **Mohammed Mufadhe Alanazi:** Conceptualization, Methodology, Software, Data curation, Writing – original draft. **Syed Sarim Imam:** Conceptualization, Methodology, Software, Data curation, Writing – original draft. **Sultan Alshehri:** Supervision, Visualization, Writing – review & editing. **Afzal Hussain:** Data curation, Writing – original draft. **Mohammad A. Altamimi:** Supervision, Visualization, Writing – review & editing. **Sulaiman S. Alhudaithi:** Data curation, Writing – original draft.

#### Declaration of Competing Interest

The authors declare that they have no known competing financial interests or personal relationships that could have appeared to influence the work reported in this paper.

#### Data availability

Data will be made available on request.

#### Acknowledgement

The authors extend their appreciation to the Deputyship for Research and Innovation, Ministry of Education in Saudi Arabia for funding this research (IFKSUOR3-473-1).

#### References

Barillaro, V., Ziemons, E., Evard, B., 2004. Effect of acidic ternary compounds on the formation of miconazole/cyclodextrin inclusion complexes by means of supercritical carbon dioxide. *J. Pharm. Sci.* 7, 378–388. PMID: 15576020.

Belgamwar, K.V., Kulkarni, A.D., 2017. Inclusion complex of chrysin with sulfobutyl ether- $\beta$ -cyclodextrin (Captisol®): Preparation, characterization, molecular modeling and in vitro anticancer activity. *J. Mol. Struct.* 1128, 563–571. <https://doi.org/10.1016/j.molstruc.2016.09.025>.

Bera, H., Chekuri, S., Sarkar, S., Kumar, S., Muvva, N.B., Mothe, S., Nadimpalli, J., 2016. Novel pimozone- $\beta$ -cyclodextrin-polyvinylpyrrolidone inclusion complexes for

Tourette syndrome treatment. *J. Mol. Liq.* 215, 135–143. <https://doi.org/10.1016/j.molliq.2015.12.054>.

Brewster, M.E., Loftsson, T., 2007. Cyclodextrins as pharmaceutical solubilizers. *Adv. Drug Deliv. Rev.* 59 (7), 645–666. <https://doi.org/10.1016/j.addr.2007.05.012>.

Crini, G., Fourmentin, S., Fenyvesi, E., 2018. Cyclodextrins, from molecules to applications. *Environ. Chem. Lett.* 16, 1361–1375. <https://doi.org/10.1007/s10311-018-0763-2>.

da Silva Mourao, L.C., Batista, D.R.M.R., Honorato, S.B., Ayala, A.P., Morais, W.A., Barbosa, E.G., Raffin, F.N., de Lima Moura, T.F.A., 2016. Effect of hydroxypropyl methylcellulose on beta cyclodextrin complexation of praziquantel in solution and in solid state. *J. Incl. Phenom. Macrocycl. Chem.* 85, 151–160. <https://doi.org/10.1007/s10847-016-0614-3>.

de Melo, P.N., Barbosa, E.G., Garnero, C., de Caland, L.B., Matheus, Pedrosa F.F., Longhi, M.R., da Silva-Júnior, A.A., 2016. Interaction pathways of specific co-solvents with hydroxypropyl- $\beta$ -cyclodextrin inclusion complexes with benznidazole in liquid and solid phase. *J. Mol. Liq.* 223, 350–359. <https://doi.org/10.1016/j.molliq.2016.08.042>.

De Miranda, C., Azevedo-Martins, E., Veiga, F., Humberto, F., 2011. Cyclodextrins and ternary complexes: technology to improve solubility of poorly soluble drugs. *Brazilian J. Pharm. Sci.* 47, 665–681. <https://doi.org/10.1590/S1984-82502011000400003>.

Fatani, W.K., Aleanizy, F.S., Alqahtani, F.Y., Alanazi, M.M., Aldossari, A.A., Shakeel, F., Haq, N., Abdelhady, H., Alkahtani, H.M., Alsarra, I.A., 2023. Erlotinib loaded dendrimer nanocomposites as a targeted lung cancer chemotherapy. *Molecules* 28, 3974. <https://doi.org/10.3390/molecules28093974>.

Fenyvesi, F., Nguyen, P., Haimhofer, A., Rusznyak, A., Vasvari, G., Bacskay, I.L., Vecsernyes, M., Ignat, S.M., Dinescu, S., Costache, M., Ciceu, A., Hermenean, A., Varadi, J., 2020. Cyclodextrin complexation improves the solubility and Caco-2 permeability of chrysin. *Materials* 13, 3618. <https://doi.org/10.3390/ma13163618>.

Figueiras, J.M., Sarragaça, A.A., Pais, R.A., Carvalho, J.F. Veiga, 2010. The Role of L-arginine in inclusion complexes of omeprazole with cyclodextrins. *AAPS Pharm. Sci. Tech.* 11, 233–240. <https://doi.org/10.1208/s12249-009-9375-2>.

Gonzalez, C.A., Riboli, E., 2010. Diet and cancer prevention: contributions from the European prospective investigation into cancer and nutrition (EPIC) study. *Eur. J. Cancer* 46, 2555–2562. <https://doi.org/10.1016/j.ejca.2010.07.025>.

Higuchi, T., Connors, K.A., 1965. Phase solubility techniques. *Adv. Anal. Chem. Instrum.* 4, 117–212.

Imam, S.S., Alshehri, S., Mahdi, W.A., Alotaibi, A.M., Alhwaifi, M.H., Hussain, A., Altamimi, M.A., Qamar, W., 2022. Formulation of Multicomponent Chrysin-Hydroxy Propyl  $\beta$  Cyclodextrin-Poloxamer Inclusion complex using Spray Dry Method: Physicochemical Characterization to Cell Viability Assessment. *Pharmaceuticals* 15, 1525. <https://doi.org/10.3390/ph15121525>.

Jug, M., Mennini, N., Kover, K.E., Mura, P., 2014. Comparative analysis of binary and ternary cyclodextrin complexes with econazole nitrate in solution and in solid state. *J. Pharm. Biomed. Anal.* 91, 81–91. <https://doi.org/10.1016/j.jpba.2013.12.029>.

Khoo, B.Y., Chua, S.L., Balaram, P., 2010. Apoptotic Effects of Chrysin in Human Cancer Cell Lines. *Int. J. Mol. Sci.* 11, 2188–2199. <https://doi.org/10.3390/ijms11052188>.

Khushbu, Jindal R., 2022. Cyclodextrin mediated controlled release of edaravone from pH-responsive sodium alginate and chitosan-based nanocomposites. *Int. J. Biol. Macromol.* 202, 11–25. <https://doi.org/10.1016/j.jbiomac.2022.01.001>.

Lavania, K., Garg, A., 2023. Inclusion complex of chrysin with Hydroxypropyl- $\beta$ -cyclodextrin (HP- $\beta$ -CD) preparation, characterization, and dissolution Study. *Bio. Nano Sci.* 13, 616–624. <https://doi.org/10.1007/s12668-023-01106-0>.

Li, L., Ma, P., Cao, Y., Tao, L., Tao, Y.J., 2011. Single-dose and multiple-dose pharmacokinetics of zaltoprofen after oral administration in healthy chinese volunteers. *Biomed. Res.* 25, 56–62. [https://doi.org/10.1016/S1674-8301\(11\)60007-9](https://doi.org/10.1016/S1674-8301(11)60007-9).

Lim, W., Ryu, S., Bazer, F.W., Kim, S.M., Song, G., 2018. Chrysin attenuates progression of ovarian cancer cells by regulating signaling cascades and mitochondrial dysfunction. *J. Cell. Physiol.* 233 (4), 3129–3140. <https://doi.org/10.1002/jcp.26150>.

Mennini, N., Maestrelli, F., Cirri, M., Mura, P., 2016. Analysis of physicochemical properties of ternary systems of oxaprozin with randomly methylated- $\beta$ -cyclodextrin and l-arginine aimed to improve the drug solubility. *J. Pharm. Biomed. Anal.* 129, 350–358. <https://doi.org/10.1016/j.jpba.2016.07.024>.

Mura, P., Bettinetti, G., Cirri, M., Maestrelli, F., Sorrenti, M., Catenacci, L., 2005. Solid-state characterization and dissolution properties of naproxen arginine-hydroxypropyl-beta-cyclodextrin ternary system. *Eur. J. Pharm. Biopharm.* 59, 99–106. <https://doi.org/10.1016/j.ejpb.2004.05.005>.

Pan, M.H., Ho, C.T., 2008. Chemopreventive effects of natural dietary compounds on cancer development. *Chem. Soc. Rev.* 37, 2558–2574. <https://doi.org/10.1039/b801558a>.

Parajuli, P., Joshee, N., Rimando, A.M., Mittal, S., Yadav, A.K., 2009. *In vitro* anti-tumor mechanisms of various Scutellaria extracts and constituent flavonoids. *Planta Med.* 75 (75), 41–48. <https://doi.org/10.1055/s-0028-1088364>.

Przybyla, M.A., Yilmaz, G., Becer, C.R., 2020. Natural cyclodextrins and their derivatives for polymer synthesis. *Polym. Chem.* 11 (48), 7582–7602. <https://doi.org/10.1039/D0PY01464H>.

Redenti, E., Szente, L., Szejtli, J., 2001. Cyclodextrin complexes of salts of acidic drugs. Thermodynamic properties structural features, and pharmaceutical applications. *J. Pharm. Sci.* 90, 979–986. <https://doi.org/10.1002/jps.1050>.

Ribeiro, L., Loftsson, T., Ferreira, D., Veiga, F., 2003. Investigation and physicochemical characterization of vinpocetine-sulfobutyl ether  $\beta$ -cyclodextrin binary and ternary complexes. *Chem. Pharm. Bull.* 51 (51), 914–922. <https://doi.org/10.1248/cpb.51.914>.

- Sami, F., Philip, B., Pathak, K., 2010. Effect of Auxiliary Substances on Complexation Efficiency, and Intrinsic Dissolution Rate of Gemfibrozil- $\beta$ -CD Complexes. *AAPS Pharm. Sci. Tech.* 11, 27–35. <https://doi.org/10.1208/s12249-009-9350-y>.
- Sherje, A.P., Kulkarni, V., Murahari, M., Nayak, U.Y., Bhat, P., Suvarna, V., Dravyakar, B., 2017. Inclusion complexation of etodolac with Hydroxypropyl- $\beta$ -cyclodextrin and auxiliary Agents: Formulation characterization and molecular modeling studies. *Mol. Pharm.* 14, 1231–1242. <https://doi.org/10.1021/acs.molpharmaceut.6b01115>.
- Sherje, A.P., Patel, F., Murahari, M., Suvarna, V., Patel, K., 2018. Study on effect of L-arginine on solubility and dissolution of Zaltoprofen: Preparation and characterization of binary and ternary cyclodextrin inclusion complexes. *Chem. Phys. Lett.* 694, 120–128. <https://doi.org/10.1016/j.cplett.2018.01.025>.
- Song, S., Gao, K., Niu, R., Wang, J., Zhang, J., Gao, C., Yang, B., Liao, X., 2020. Inclusion complexes between chrysin and amino-appended  $\beta$ -cyclodextrins (ACDs): Binding behavior, water solubility, in vitro antioxidant activity and cytotoxicity. *Mater. Sci. Eng. C* 106, 110161. <https://doi.org/10.1016/j.msec.2019.110161>.
- Suvarna, V., Kajwe, A., Murahari, M., Pujar, G.V., Inturi, B.K., Sherje, A.P., 2017. Inclusion Complexes of Nateglinide with HP- $\beta$ -CD and L-Arginine for Solubility and Dissolution Enhancement: Preparation, Characterization, and Molecular Docking Study. *J. Pharm. Innov.* 12, 168–181. <https://doi.org/10.1007/s12247-017-9275-z>.
- Suvarna, V., Thorat, S., Nayak, U., Sherje, A., Murahari, M., 2018. Host-guest interaction study of Efavirenz with hydroxypropyl- $\beta$ -cyclodextrin and L-arginine by computational simulation studies: Preparation and characterization of supramolecular complexes. *J. Mol. Liq.* 259, 55–64. <https://doi.org/10.1016/j.molliq.2018.02.131>.
- Tiwari, G., Tiwari, R., Rai, A.K., 2010. Cyclodextrins in delivery systems: applications. *J. Pharm. Bioall. Sci.* 2, 72–79. <https://doi.org/10.4103/0975-7406.67003>.
- Wang, D., Li, H., Gu, J., Guo, T., Yang, S., Guo, Z., Zhang, X., Zhu, W., Zhang, J., 2013. Ternary system of dihydroartemisinin with hydroxypropyl- $\beta$ -cyclodextrin and lecithin: simultaneous enhancement of drug solubility and stability in aqueous solutions. *J. Pharm. Biomed. Anal.* 83, 141–148. <https://doi.org/10.1016/j.jpba.2013.05.001>.
- Xiao, Q.Z., Sheng, M.P., Chang, P.H., Tan, L.F., Yuan, Q., Deng, H.W., Li, Y.J., 2010. Synthesis characterization and vasculoprotective effects of nitric-oxide-donating derivatives of chrysin. *Bioorg. Med. Chem.* 18, 3020–3025. <https://doi.org/10.1016/j.bmc.2010.03.056>.
- Yokoo, M., Kubota, Y., Motoyama, K., Higashi, T., Taniyoshi, M., Tokumaru, H., Nishiyama, R., Tabe, Y., Mochinaga, S., Sato, A., Sueoka-Aragane, N., Sueoka, E., Arima, H., Irie, T., Kimura, S., 2015. 2-Hydroxypropyl- $\beta$ -Cyclodextrin Acts as a Novel Anticancer Agent. *PLoS One* 10 (11), e0141946. <https://doi.org/10.1371/journal.pone.0141946>.
- Zhu, Z.Y., Luo, Y., Liu, Y., Wang, X.T., Liu, F., Guo, M.Z., Wang, Z., Liu, A.J., Zhang, Y.M., 2016. Inclusion of chrysin in  $\beta$ -cyclodextrin and its biological activities. *J. Drug Del. Sci. and Tech.* 31, 176–186. <https://doi.org/10.1016/j.jddst.2016.01.002>.